Kovove Mater. 52 2014 35–45
DOI: 10.4149/km_2014_1_35

Adsorption and corrosion inhibitive properties of 2-Mercaptobenzothiazole on AISI steel 4130 alloy in hydrochloric acid solution

A. R. Hoseizadeh, I. Danaee*, M. H. Maddahy

Abadan Faculty of Petroleum Engineering, Petroleum University of Technology, P.O. Box 619-63187-14331 Abadan, Iran

Received 5 February 2012, received in revised form 27 September 2013, accepted 27 September 2013

Abstract

The inhibition ability of 2-Mercaptobenzothiazole (MBT) against the corrosion of AISI steel 4130 in 1 M HCl solution was evaluated by polarization, electrochemical impedance spectroscopy (EIS) and chronoamperometry. Polarization studies indicated that MBT retarded both the cathodic and anodic reactions through chemical adsorption and blocking the active corrosion sites. The adsorption of this compound obeyed the Langmuir adsorption isotherm. The inhibition efficiency was increased with inhibitor concentration as well as temperature. EIS data was analyzed for an equivalent circuit model and showed that as the inhibitor concentration increased the charge transfer resistance of steel increased whilst double layer capacitance decreased. Kinetic and thermodynamic parameters such as activation energy, enthalpy, entropy and free energy of activation and adsorption were calculated. Atomic force microscopy (AFM) and optical microscope were used to study the steel surface with and without inhibitor.

K e y w o r d s: steel 4130, corrosion, inhibitor, adsorption isotherm, Langmuir

1. Introduction

The survey of steel corrosion in acidic environments has turned into an important subject because of the widened industrial utilization of acid solutions. Such as the refining of crude oil that makes a wide variety of corrosive media. Refinery corrosion is typically caused by a strong acid aggressing the surface of equipments [1]. Generally, hydrochloric acid solutions are used for pickling, chemical and electrochemical etching of some metals and alloys [2]. Hot acid solutions are mostly used for removing mill scales and rusts from the metal surfaces in different industries at raised temperatures, for example 60 ℃ in hydrochloric acid and up to 95 ℃ in sulfuric acid [3].

The use of corrosion inhibitor is one of the most important methods for protecting the surfaces of metals or alloys against corrosion and reducing the corrosion damage in acid solutions [2, 4]. An inhibitor must move water molecules from the metal surface, interact with anodic or/and cathodic reaction sites to decrease the oxidation or/and reduction corrosion reactions, and prevent transportation of water and corrosion active species on the surface. Three main types of inhibitors: organic inhibitors, inorganic inhibitors and mixed material inhibitors are widely used in acidic solutions [5, 6].

Inhibition of organic compound inhibitors is due to the interaction between inhibitor molecules and the metal surface via adsorption. The inhibitor adsorption depends on parameters such as the surface charge and nature of the metal, the inhibitor structure, aggressive media type and the extent of aggressiveness and also on the nature of its interaction with metal surface. Furthermore, it depends on the presence of heteroatoms such as phosphorus, nitrogen, oxygen, and sulphur, aromatic rings or multiple bonds. The inhibition efficiency increases in the order O < N < S < P [7].

These compounds decrease the corrosion rate by blocking the active surface sites. Four kinds of adsorption may occur by organic inhibitors at metal/solution

*Corresponding author: tel.: (0098631) 4429937; e-mail address: danaee@put.ac.ir

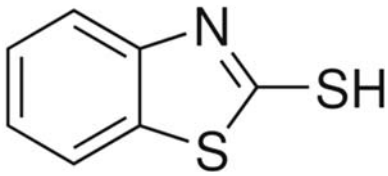

Fig. 1. Chemical structure of MBT.

interface: (i) electrostatic attraction between the charged molecules and charged metal, (ii) interaction between metal and uncharged electron pairs in the molecule, (iii) interaction between metal and p-electrons, (iiii) both of (i) and (iii) [8]. The thiazole derivatives were investigated in many works as corrosion inhibitors for steel, zinc, aluminum and its alloys in acidic solutions [9 – 11].

This work is devoted to study the inhibition characteristics of MBT (a derivative of thiazole) as an inhibitor for carbon steel in HCl solution, using potentiodynamic polarization measurements (Tafel), electrochemical impedance spectroscopy (EIS), chronoamperometry and observation of surface topography by atomic force microscopy (AFM) and optical microscope.

2. Materials and methods

2.1. Materials

Materials used in this work were Merck products of analytical grade and were used without further purifications. For study of the effectiveness of MBT inhibitor AISI steel 4130 cylinders were pressed into Teflon holders playing the role of working electrodes. The working area was 0.78 cm^2 and remained exactly fixed in contact with aggressive solution. Then, they were mechanically polished with various grade emery papers (400, 600, 800, and 1200), and consequently washed in acetone and double distilled water and finally dried by dry air and then placed in beakers containing 1 M HCl solution.

The chemical composition of the steel 4130 samples (wt.%) was distinguished by SPECTROLAB quantometer (C: 0.2, Si: 0.13, Mn: 0.69, P: 0.02, S: 0.021, Cr: 1, Ni: 0.23, Mo: 0.16, Cu: 0.22, V: 0.002, W: 0.008, Co: 0.008, Sn: 0.02, Pb: 0.002, As: 0.009, Sb: 0.005 wt.%, Fe: bal.). The molecular structure of 2-Mercaptobenzothiazole (MBT) is given in Fig. 1. Broad concentration interval was chosen where the highest concentration was bounded by the solubility of the inhibitor or by the observation of a plateau in the η versus C. The intervals of MBT were chosen 50–250 ppm up to solution limit. The acid solutions (1 M HCl) were made from 37 % HCl stock solution using double-distilled water.

2.2. Methods

Computer controlled ZAHNER Elektrik model IM6Ex potentiostat was used for electrochemical measurements. THALES software was employed for assessing the experimental data. A three-electrode arrangement consisting of steel 4130 as working electrode, a platinum as counter electrode, and a saturated calomel electrode (SCE) as a reference was used. The electrochemical tests were conducted at 25 ℃, 45 ℃ and 65 ℃ temperatures.

For polarization measurements, the potential was scanned with a scan rate of 1 mV s^{-1} from −800 mV to −200 mV vs. SCE. Cathodic and anodic Tafel slops (β_c and β_a) were calculated from the Tafel regions of cathodic and anodic branch of polarization curves, respectively. Before recording the polarization data, working electrode was maintained at its corrosion potential for 30 min until a steady state was obtained.

Frequency ranging of EIS experiments was carried over the frequency range from 100 kHz to 30 mHz and peak-to-peak A.C. amplitude of 10 mV. The impedance diagrams were plotted in the Nyquist representation. The results were used to achieve the equivalent circuit. Fitting of experimental impedance spectroscopy data to the proposed equivalent circuit was done by means of a home written least square software based on the Marquardt method for the optimization of functions and Macdonald weighting for the real and imaginary parts of the impedance [12, 13].

The surface morphology of steel specimens after 6 h placing in 1 M HCl in the absence and presence of MBT were studied using Nanosurf easy Scan 2 AFM and optical microscope.

3. Results and discussion

3.1. Polarization measurements and effect of temperature

Figures 2a,b,c show the cathodic and anodic polarization curves of steel immersed in 1 M HCl in the absence and presence of different concentrations of the inhibitor and at different temperatures. As it can be obviously seen from these Figs., the addition of MBT to the corrosive media slows down both cathodic hydrogen evolution reactions and anodic dissolution of steel. The corrosion current density and corrosion rate of steel noticeably reduced in the presence of the inhibitor. The inhibition of both anodic and cathodic reactions was more and more distinct with increasing inhibitor concentration while the corrosion potential nearly remained the same in comparison with blank solution. These results indicate that MBT can be classified as the mixed type corrosion inhibitor [14]. The cathodic branches in the presence of inhibitor give

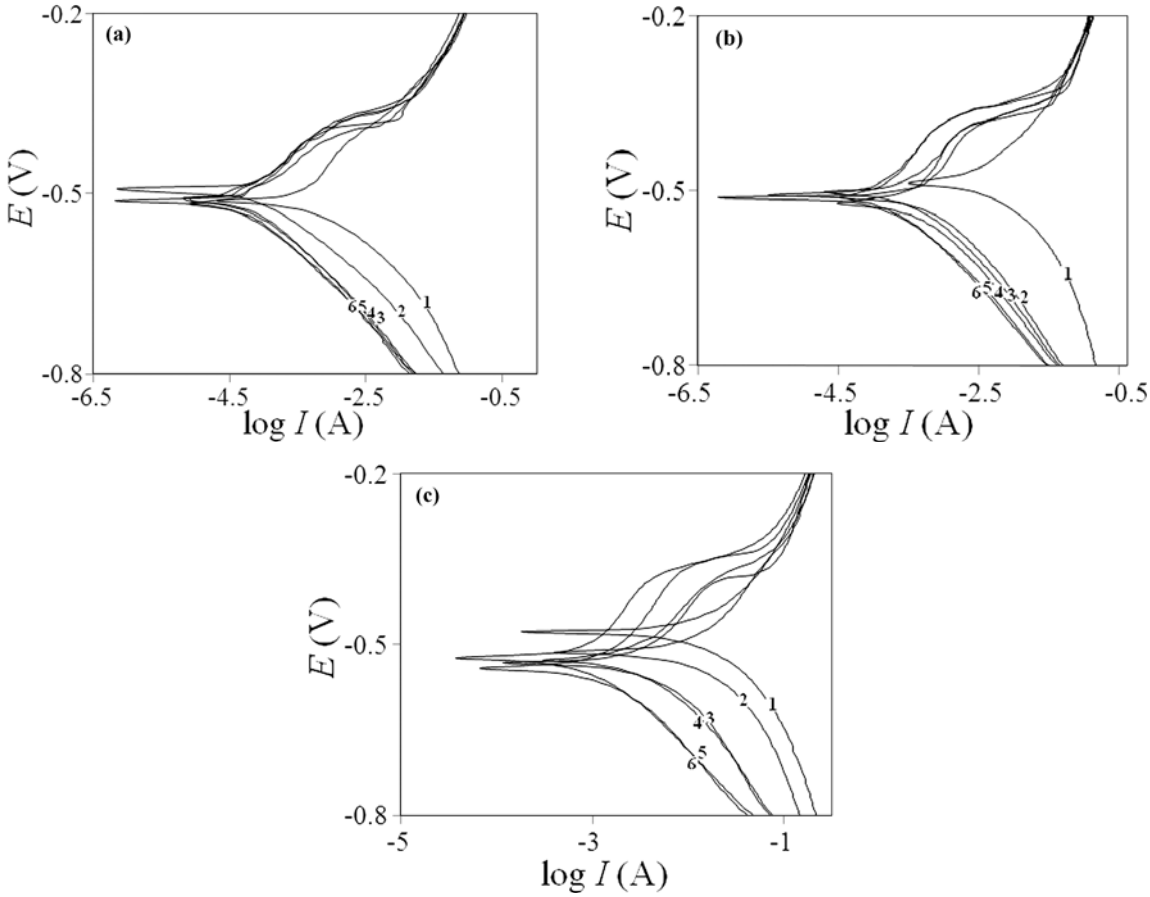

Fig. 2. Anodic and cathodic polarization curves (Tafel curves) for steel in 1 M HCl at (a) 25, (b) 45 and (c) 65 °C without and with various concentration of MBT: (1) blank, (2) 50, (3) 100, (4) 150, (5) 200 and (6) 250 ppm.

rise to parallel lines, which indicates that the increasing MBT concentration does not modify the hydrogen evolution mechanism, and the reduction of H^+ ions at steel surface is charge transfer controlled [14, 15].

In low anodic overpotentials, a significant inhibition, especially at higher inhibitor concentrations, is observed [16] which was due to strong adsorption of inhibitor and corrosion products on electrode surface. Corrosion potential (E_{corr}), current density (I_{corr}), cathodic and anodic Tafel slopes (β_c and β_a), surface coverage (θ), inhibition efficiency (η %) and polarization resistance (R_p) were calculated and listed in Table 1. The degree of surface coverage (θ) and the percentage inhibition efficiency (IE %) were calculated using the following equations [17]:

$$\text{IE } \% = \left(1 - \frac{I}{I_0}\right) \times 100, \tag{1}$$

$$\theta = \left(1 - \frac{I}{I_0}\right), \tag{2}$$

where I_0 and I are the corrosion current densities in the absence and presence of the inhibitor, respectively. The values of polarization resistance (R_p) were calculated from the known Stern-Geary equation [18, 19]:

$$R_p = \frac{b_a b_c}{2.303 i_{corr}(b_a + b_c)}. \tag{3}$$

The effect of temperature on the inhibited metal corrosion reaction is very complex, because many changes occur on the metal surface such as rapid desorption of inhibitor. In the presence of the inhibitor, the corrosion current of steel decreases at any given temperature as inhibitor concentration increases due to the increase of the degree of surface coverage. In contrast, at constant inhibitor concentration, the corrosion current increases with the rise of temperature. Also it can be seen that the efficiency depends on the temperature and increases with the rise of temperature. This can be explained by the increase of the strength of the adsorption process at elevated temperature and would suggest a chemical adsorption mode.

3.2. Electrochemical impedance spectroscopy

Figure 3 shows Nyquist plots recorded for the corrosion of steel in 1 M HCl solution with and

Table 1. Electrochemical parameters obtained from the polarization curves of MBT in different temperatures

Temp. (℃)	MBT (ppm)	I_{corr} (μA cm^{-2})	E_{corr} (mV)	β_c (mV dec^{-1})	β_a (mV dec^{-1})	R_p (Ω cm^2)	C.R. (mpy)	IE (%)	θ
	Blank	459.6	–513.5	71.5	157	46.41	210.9	–	–
	50	120	–493.5	92.8	123	91.39	55.08	73.9	0.739
25	100	92.06	–511.9	111	104	253.2	42.25	80	0.80
	150	71.05	–509.3	106	109	328.4	32.61	84.5	0.845
	200	63.38	–518	99.6	114	364.2	29.09	86.2	0.862
	250	54.74	–513.3	88.7	100	372.9	25.12	88.1	0.881
	Blank	4444	–477	120	129	6.074	2040	–	–
	50	700	–511.6	119	183	44.73	321	84.2	0.842
45	100	488	–503.7	115	147	57.41	224	89	0.89
	150	212.4	–519.8	104	153	126.6	97.50	95.2	0.952
	200	176	–510	96.4	139	140.4	80.77	96	0.96
	250	133.3	–504.2	94	118	170.4	61.19	97	0.97
	Blank	23×10^3	–474.4	218	215	2.039	10580	–	–
	50	6×10^3	–513	188	228	7.448	2758	73.9	0.739
65	100	4.3×10^3	–538.7	125	219	8.035	1974	81.3	0.813
	150	2.5×10^3	–532.4	127	210	13.641	1156	89.1	0.891
	200	1.6×10^3	–541.3	153	203	22.549	771.3	92.7	0.927
	250	1.3×10^3	–520.1	149	220	28.094	630.6	94	0.94

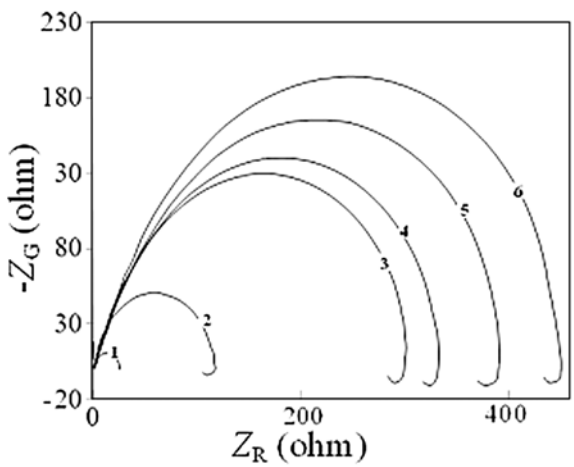

Fig. 3. Nyquist plots for steel in 1 M HCl containing different concentrations of MBT at 25℃: (1) blank, (2) 50, (3) 100, (4) 150, (5) 200 and (6) 250 ppm.

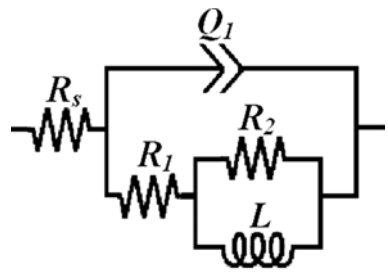

Fig. 4. Equivalent circuit compatible with the experimental impedance data in Fig. 3 for corrosion of steel electrode for different inhibitor concentrations.

without different concentrations of inhibitor obtained at E_{corr}. The Nyquist diagrams show one capacitive loop at high frequencies and one inductive loop at low-frequency values (two time constants). The first capacitive loop, at high frequencies, arises from the time constant of the electrical double layer and charge transfer resistance. The presence of the low frequencies inductive loop may be attributed to the relaxation process obtained by adsorption species like Cl^-_{ads} and H^+_{ads} on the electrode surface [20–23]. In other words, the inductive behaviour at low frequency is probably due to the consequence of the layer stabilization by products of the corrosion reaction on the electrode surface (for example, $[FeOH]_{ads}$ and $[FeH]_{ads}$) involving inhibitor molecules and their reactive products [21]. It may also be attributed to the re-dissolution of the passivated surface at low frequencies [23].

The impedance of the inhibited steel increases with increasing the inhibitor's concentration and consequently the inhibition efficiency increases. These diagrams have similar shape; the shape is maintained throughout all tested concentrations, indicating that almost no change in the corrosion mechanism occurs due to the inhibitor addition. The equivalent circuit compatible with the Nyquist diagram recorded in the presence of inhibitor was depicted in Fig. 4. To obtain a satisfactory impedance simulation of stainless steel corrosion it is necessary to replace the capacitor, C, with a constant phase element (CPE) Q in the equivalent circuit. The most widely accepted explanation for the emergence of CPE behaviour, depressed

Table 2. Impedance data for steel in 1 M HCl solution without and with different concentration of inhibitor at 25 ℃

Concentration (ppm)	R_s (Ω)	R_{ct} (Ω)	$Q_{dl} \times 10^4$ (F)	n	$C_{dl} \times 10^3$ (F)	τ (s)	R_L (Ω)	L (H)
Blank	1.5	23	29	0.87	27	0.62	2	15
50	1.5	104	13	0.89	13	1.4	18.5	35
100	1.6	275	5	0.88	5	1.44	40	108
150	1.5	302	4	0.88	4.1	1.23	45	128
200	1.6	352	3	0.89	3	1.1	55	125
250	1.6	407	3	0.91	3	1.24	62	105

semicircles, is the microscopic roughness on solid electrodes causing an inhomogeneous distribution in the solution resistance as well as in the double-layer capacitance [24, 25]. The impedance of the CPE is defined as $Z_{CPE} = 1/Q(\mathrm{i}w)^n$, where Q is a capacitive parameter related to the average double layer capacitance (C_{dl}), and n is a dimensionless parameter related to the constant phase angle. In equivalent electrical circuit, R_s, CPE_{dl} and R_{ct} represent solution resistance, a constant phase element corresponding to the double layer capacitance and the charge transfer resistance. L and R_L are the inductive elements related to the relaxation process.

The simplest approach requires the theoretical transfer function $Z(\omega)$ to be represented by:

$$Z(\omega) = R_s + \frac{R_{ct}}{\dfrac{1}{1 + (Z_L(\omega)/R_{ct})} + (\mathrm{i}\omega R_{ct} Q_{dl})^n},$$
$$Z_L(\omega) = \frac{\mathrm{i}\omega R_L L}{\mathrm{i}\omega L + R_L}, \tag{4}$$

where ω is the frequency in rad s^{-1}, $\omega = 2\pi f$ and f is frequency in Hz. To corroborate the equivalent circuit, the experimental data are fitted to equivalent circuit and the circuit elements are obtained. Table 2 illustrates the equivalent circuit parameters for the impedance spectra of corrosion of steel in 1 M HCl solution. The results demonstrate that the presence of inhibitor enhances the value of R_{ct} obtained in the pure medium while that of Q_{dl} is reduced. The decrease in Q_{dl} values was caused by adsorption of inhibitor indicating that the exposed area decreased. On the other hand, a decrease in Q_{dl}, which can result from a decrease in local dielectric constant and/or an increase in the thickness of the electrical double layer, suggests that inhibitor acts by adsorption at the metal-solution interface and the formation of a protective layer on the electrode surface [26]. The thickness of this protective layer increases with increase in inhibitor concentration, since more inhibitor will electrostatically adsorb on the electrode surface. This trend is in accordance with Helmholtz model, given by the following equation [27]:

$$C_{dl} = \frac{\varepsilon_0 \varepsilon S}{e}, \tag{5}$$

where e is the thickness of the protective layer, ε is the dielectric constant of the medium, ε_0 is the vacuum permittivity and S is the effective surface area of the electrode.

As the Q_{dl} exponent (n) is a measure of the surface heterogeneity, value of n indicates that the steel surface becomes more and more homogeneous as the concentration of inhibitor increases as a result of its adsorption on the steel surface and corrosion inhibition. The increase in values of R_{ct} and the decrease in values of Q_{dl} with increasing the concentration also indicate that inhibitor acts as primary interface inhibitor and the charge transfer controls the corrosion of steel under the open circuit conditions.

In order to calculate and compare the time constants [28], the CPE values were transformed into a pure capacitance (C) using equation:

$$Q = R^{n-1} C^n. \tag{6}$$

A time constant τ was calculated using:

$$\tau = RC. \tag{7}$$

In the HCl solutions, the mean value for the time constant was increased in presence of inhibitor. Therefore, equivalent circuit could be associated with slow charging/discharging processes in presence of inhibitor [29].

3.3. Adsorption isotherm behaviour

On the progress of the corrosion reactions of steel in HCl solution, the temperature plays an important role. As the temperature increases, the energy of the reactants increases to form the activated complex which dissociates to yield the corrosion products [30]. Basic thermodynamic information on interaction between metal surface and inhibitor molecules can be provided by adsorption isotherm that employed for thermodynamic calculations of inhibitor adsorption [31]. There are different adsorption isotherms such as Langmuir, Temkin, Ei-Away, Bockris--Swinkels, Flory-Huggins and Frumkin [32]. Using thermodynamic data attained from isotherms can help to distinguish the kind of adsorption of inhibitor

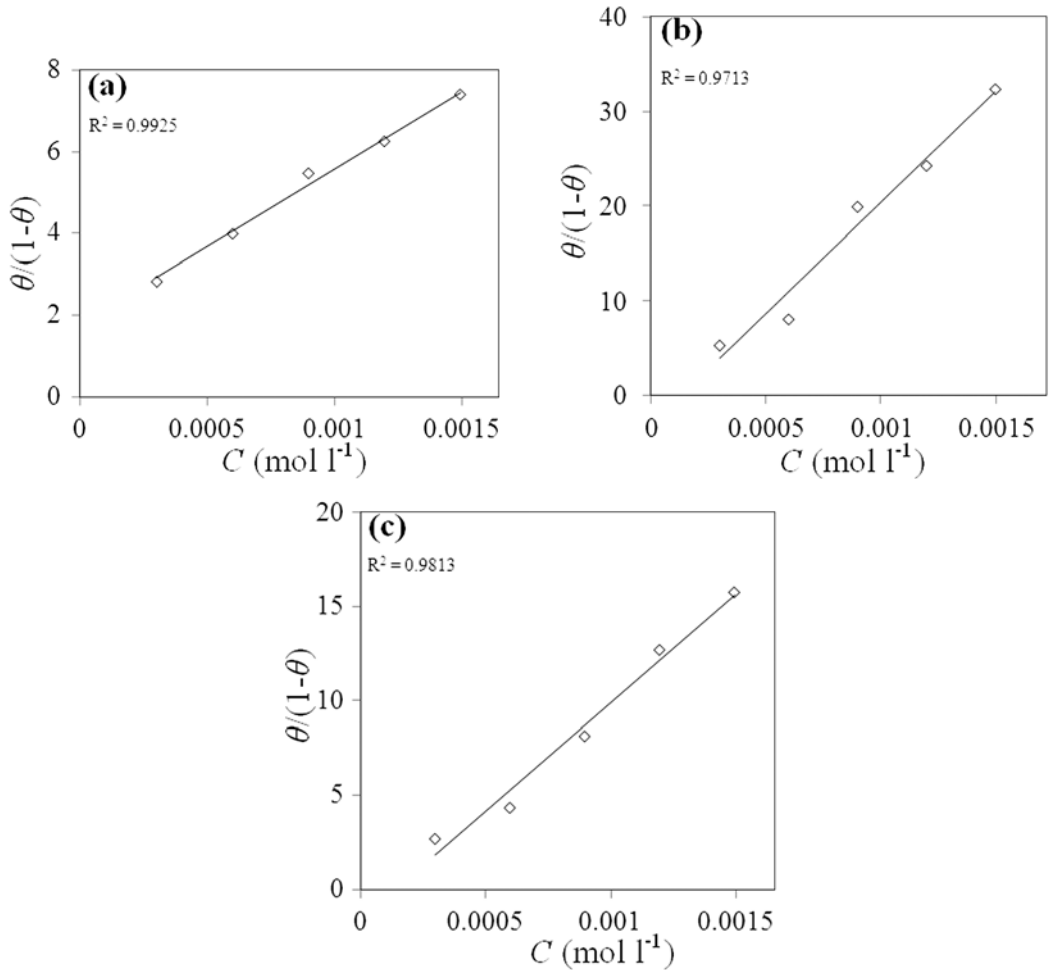

Fig. 5. Langmuir adsorption isotherm ($\theta/(1-\theta)$ vs. C) of inhibitor in 1 M HCl at (a) 25, (b) 45, and (c) 65 °C.

(chemisorption or physisorption). Organic inhibitors adsorption at the metal/solution interface can be illustrated by exchange of water molecules with inhibitor molecules on the metal surface [33]:

$$\mathrm{Org}_{(\mathrm{sol})} + x\mathrm{H_2O}_{(\mathrm{ads})} \rightleftharpoons \mathrm{Org}_{(\mathrm{ads})} + x\mathrm{H_2O}_{(\mathrm{sol})}. \quad (8)$$

In this formula, $\mathrm{Org}_{(\mathrm{sol})}$ is inhibitor of molecules dissolved in solution and $\mathrm{Org}_{(\mathrm{ads})}$ is inhibitor of molecules adsorbed on metal surface. Also, $\mathrm{H_2O}_{(\mathrm{sol})}$ and $\mathrm{H_2O}_{(\mathrm{ads})}$ are water molecule and adsorbed water molecule on metal surface in solution, respectively, and x is size ratio which represents the number of water molecules that substitute with inhibitor molecules.

The experimental data attained from polarization information could be fitted by Langmuir adsorption isotherm according to this equation [34]:

$$\frac{\theta}{1-\theta} = K_{\mathrm{ads}}C, \quad (9)$$

where θ is the surface coverage, K_{ads} is the adsorption-desorption equilibrium constant, C is the inhibitor concentration.

As seen from Figs. 5a,b,c, the plot of $\theta/(1-\theta)$ versus C yields a straight line with a correlation coefficient more than 0.97, showing that the adsorption of these inhibitors in acidic solution is fitted to Langmuir adsorption isotherm. This adsorption isotherm represents that there are no interactions with other adsorbed species and adsorbed molecules occupy only one site on the metal surface [35, 36].

To calculate activation parameters for the corrosion process, Arrhenius (Eq. (10) and transition state Eq. (11)) employed [37]:

$$I_{\mathrm{corr}} = A\exp\left(-\frac{E_{\mathrm{a}}}{RT}\right), \quad (10)$$

$$I_{\mathrm{corr}} = \frac{RT}{Nh}\exp\left(-\frac{\Delta H^{\circ}}{RT}\right)\exp\left(-\frac{\Delta S^{\circ}}{R}\right), \quad (11)$$

Table 3. Activation parameters of the dissolution of steel in 1 M HCl solution in the absence and presence of inhibitor in 1 M HCl

MBT conc. (ppm)	E_a (kJ mol^{-1})	A (μA cm^{-2})	ΔH° (kJ mol^{-1})	ΔS° (kJ mol^{-1} K^{-1})	ΔG° (kJ mol^{-1})		
					25 °C	45 °C	65 °C
Blank	82.20	1.23×10^{17}	79.57	0.0733	57.7	56.23	54.77
50	81.72	2.24×10^{16}	79.10	0.0591	61.45	60.27	59.1
100	80.22	9.22×10^{15}	77.58	0.0519	62.11	61.07	60.03
150	77.67	2.16×10^{15}	71.44	0.0279	63.09	62.54	61.98
200	67.48	3.37×10^{13}	65.41	0.0071	63.29	63.14	63
250	63.04	4.8×10^{12}	64.16	0.0013	63.75	63.73	63.70

where I_{corr} is the corrosion rate, A is the Arrhenius pre-exponential factor, E_a is the activation energy for corrosion process, h is the Planck's constant, N is the Avogadro's number, R is the gas constant, T is the absolute temperature, ΔH° is the enthalpy, and ΔS° is the entropy of activation. A fitted straight line is obtained for the plot of $\ln I_{corr}$ versus $1/T$, Fig. 6. The activation energies (E_a) at different concentrations of inhibitor were determined by linear regression of these graphs. The results are listed in Table 3. Radovici reported that inhibitors for which E_a is smaller in the presence of inhibitor than in the absence of that in the solution undergo chemisorption [38]. The chemical adsorption is due to formation of coordinated bond between the d-orbital of iron and inhibitor molecules on the surface of steel through lone pair of electron of N, S and O atoms [39]. Szauer and Brand explained that the decrease in activation energy can be referred to a considerable increase in the adsorption of the inhibitor on the steel surface with increase in temperature. As more adsorption of inhibitor molecules occurs, desorption decreases because these two opposite processes are in equilibrium. More adsorption of inhibitor molecules at higher temperatures makes the lower surface area of steel exposes in contact with acid environment, resulting decreased corrosion rates with increase in temperature [40].

A study of Table 3 shows that values of E_a in 1 M HCl containing MBT are lower than that in uninhibited solution (82.2 kJ mol^{-1}). Increasing of inhibitor efficiency and decreasing in the apparent activation energy reveals chemical adsorption. Furthermore, decrease in A reduces the corrosion rate of the carbon steel. So, the corrosion rate of steel decreased with increasing the inhibitor concentration [41].

Plotting $\log(I_{corr}/T)$ versus $(2.303RT)^{-1}$ is showed in Fig. 7. In these plots the straight lines are obtained with a slope ($-\Delta H^\circ$) and an intercept of $\left(\log\frac{R}{Nh} - \frac{\Delta S^\circ}{2.303R}\right)$ from which the values of ΔH° and ΔS° can be calculated that are given in Table 3. Investigation of these data shows that the

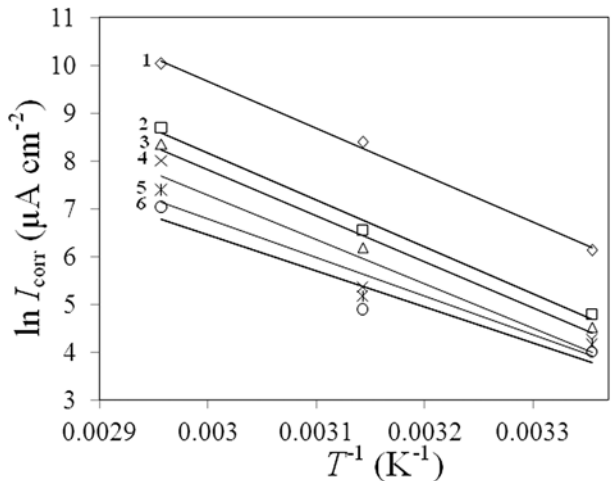

Fig. 6. Arrhenius plot for steel corrosion in 1 M HCl in the absence and presence of different concentrations of MBT: (1) blank, (2) 50, (3) 100, (4) 150, (5) 200 and (6) 250 ppm.

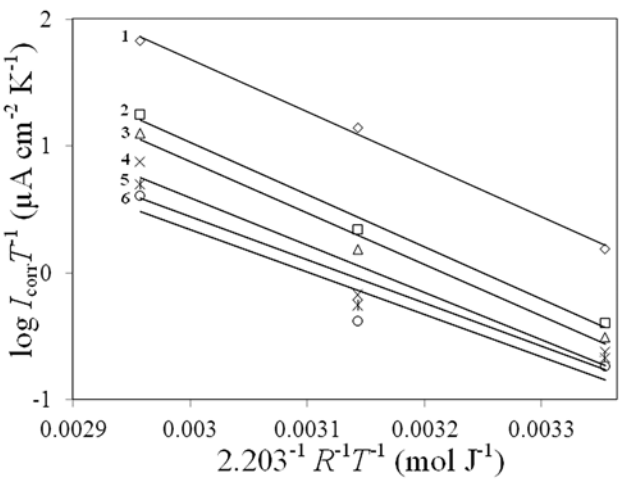

Fig. 7. Transition state plot for steel corrosion in 1 M HCl in the absence and presence of different concentrations of MBT: (1) blank, (2) 50, (3) 100, (4) 150, (5) 200 and (6) 250 ppm.

Table 4. Thermodynamic and equilibrium adsorption parameters for adsorption inhibitor on steel surface in 1 M HCl solution

Different thermodynamic equations	ΔH_{ads} (kJ mol^{-1})	ΔS_{ads} (kJ mol^{-1} K^{-1})
Basic Thermodynamic Equation	22.14	0.179
Van't Half Equation	24.3	0.184
Gibbs-Helmholtz Equation	24.3	–

thermodynamic parameters (ΔH° and ΔS°) for dissolution reaction of steel in 1 M HCl in the presence of inhibitor are lower (64.16 kJ mol^{-1}, 0.0013 kJ mol^{-1}) than that in the absence of inhibitor (79.57 kJ mol^{-1}, 0.073 kJ mol^{-1}). The positive values of ΔH_a mean that the dissolution reaction is an endothermic process in HCl solution.

From the slopes of $\theta/(1-\theta)$ versus C lines, K_{ads} values can be obtained. K_{ads} is related to the standard free energy of adsorption with the following equation [36]:

$$\Delta G^\circ_{ads} = -RT\ln(55.5K_{ads}). \tag{12}$$

By using Eq. (12), the calculated ΔG°_{ads} at 65 ℃ is −37.6 kJ mol^{-1}. The negative sign of ΔG° and high value of K_{ads} indicates that MBT molecules adsorbed strongly and immediately on the steel surface [42]. Usually, the magnitude of standard free energy of adsorption around −20 kJ mol^{-1} or less negative is considered for electrostatic interactions between inhibitor molecules and charged metal surface (i.e., physisorption). The magnitude of ΔG° near −40 kJ mol^{-1} or more negative is usually assumed for charge sharing or transferring from organic molecules to the metal surface to form a coordinate type of metal bond (i.e., chemisorption) [36]. In this work, ΔG°_{ads} is a negative value and near −40 kJ mol^{-1}, so the adsorption process is chemisorption.

In acidic solution, nitrogen atom in thiazole ring can be protonated easily because is planar and having greater electron density. Coordinate covalent bond formation between electron pairs of unprotonated N-atom and S-atom in thiazole ring and metal surface can take place. The inhibitor has two nucleophilic centres likely to undergo a protonation in acid medium: the nitrogen and the sulphur located in the molecular structure.

Corrosion inhibition of MBT for steel can be better explained by using entropy ΔS°_{ads} and the enthalpy ΔH°_{ads} of adsorption which can be calculated from the following integrated van't Hoff equation [42]:

$$\ln K_{ads} = -\frac{\Delta H^\circ_{ads}}{RT} + \frac{\Delta S^\circ_{ads}}{R} + \ln\frac{1}{55.5}. \tag{13}$$

Enthalpy and entropy of adsorption can be obtained from plotting $\ln K_{ads}$ versus $1/T$, straight lines are attained with intercept equal to $(\Delta S^\circ_{ads}/R) + \ln(1/55.5)$ and slope equal to $-H^\circ_{ads}/R$. The calculated values of the entropy of adsorption and heat of adsorption are listed in Table 4. Also the Gibbs-Helmholtz equation can be used for calculating the enthalpy of adsorption [43]:

$$\left[\frac{\partial(\Delta G^\circ_{ads}/R)}{\partial T}\right] = -\frac{\Delta H^\circ_{ads}}{T^2}. \tag{14}$$

By integrating from Eq. (14) it can also be represented as:

$$\frac{\Delta G^\circ_{ads}}{T} = \frac{\Delta H^\circ_{ads}}{T} + K. \tag{15}$$

The obtained value of ΔH°_{ads} is given in Table 4. It can be seen that the value of enthalpy of adsorption in Gibbs-Helmholtz equation agrees with the one obtained using van't Hoff equation. Heat of adsorption (ΔH°_{ads}) and entropy of adsorption (ΔS°_{ads}) can also be found based on the following thermodynamic equation [44]:

$$\Delta G^\circ_{ads} = \Delta H^\circ_{ads} - T\Delta S^\circ_{ads}. \tag{16}$$

For this inhibitor, ΔH°_{ads} and ΔS°_{ads} values are given in Table 4. The values of thermodynamic parameters for the adsorption of inhibitors can represent beneficial information about the corrosion inhibition mechanism. An endothermic adsorption ($\Delta H^\circ_{ads} > 0$) indicates the chemical adsorption where an exothermic adsorption ($\Delta H^\circ_{ads} < 0$) may involve physical one, chemical one or a mixture of both [45]. In an exothermic process, chemisorption can be differentiated from physisorption by considering the absolute value of ΔH°_{ads}. According to Table 4, the positive sign of ΔH°_{ads} shows that the adsorption of inhibitor is endothermic and indicating that it is a chemical adsorption process approving previous deduction. The positive sign of ΔS°_{ads} is also related to substitutional process, which can be attributed to an increase in the solvent entropy and more positive water desorption entropy. It also can illustrate with increase of disorders due to the more water molecules which can be desorbed from the metal surface by one inhibitor molecule [46].

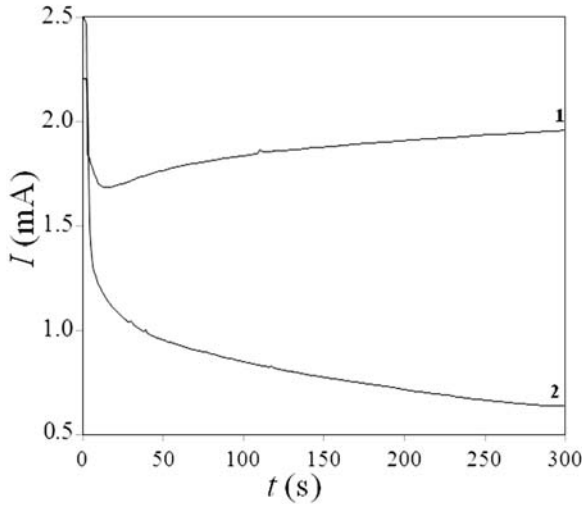

Fig. 8. Current transients of steel electrode at –0.4 V vs. SCE: (1) blank, (2) 250 ppm of MBT.

3.4. Chronoamperometry

In order to gain more insight about the effect of inhibitor on the electrochemical behavior of steel in 1 M HCl solution, potentiostatic current-time transients were recorded. Figure 8 shows the current transients of steel electrode at −0.4 V vs. SCE applied anodic potential. Initially the current decreases monotonically with time. The decrease in the current density is due to the formation of corrosion products layer on the anode surface. However, in later times the current increases tracing approximately a straight line to reach a steady state value depending on applied potential (Fig. 8). The increase in current is related to the dissolution of the steel and pit nucleation and pit growth. In presence of inhibitor, increasing current was not observed and electrode was inhibited from corrosion due to inhibitor adsorption.

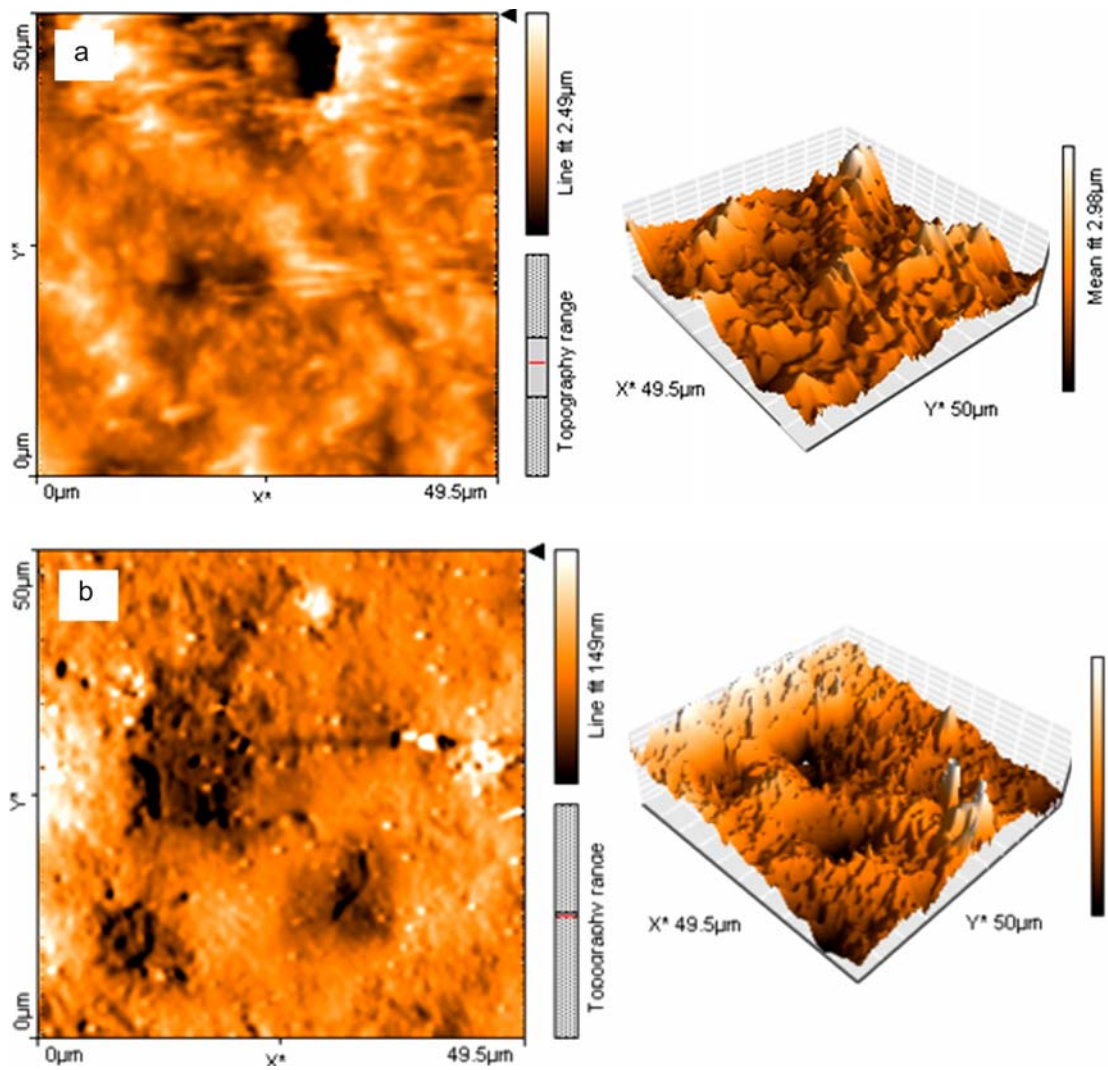

Fig. 9. AFM surface topography images immersed for 6 h in 1 M HCl: (a) in the absence of inhibitor; (b) in the presence of 250 ppm of MBT.

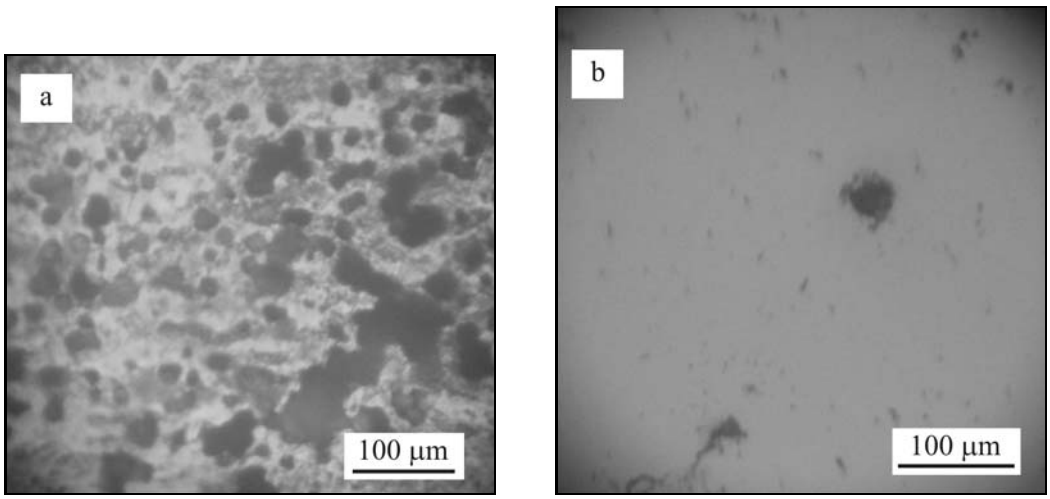

Fig. 10. Optical micrographs (400×) of the steel alloy immersed for 6 h in (a) 1 M HCl, and (b) 1 M HCl containing 250 ppm of MBT.

3.5. Surface studies

AFM provides an excellent technique of considering the surface topography. The corresponding two and three-dimensional images of corroded surface of carbon steel in the absence of inhibitor after 6 h immersion in 1 M HCl (25 ℃) are shown in Fig. 9a. These images show that the surface looks rather uneven and seems potholed shape with 2.98 µm mean roughness. The AFM images of corroded surface of carbon steel in the presence of 250 ppm of MBT are shown in Fig. 9b. As can be seen from these figures, it is obvious that the surface looks more uniform and becomes more flat than that in the absence of inhibitor with 156 nm mean roughness.

The metallographs presented in Fig. 10a,b show the morphologies of the electrode surface after 6 h immersion in 1 M HCl (25 ℃) with and without inhibitor. The sample in HCl solution shows localized attacks which appear as drastic changes of the surface (Fig. 10a), while sample immersed in the 250 ppm MBT-added solution shows smooth surface with low density of pits and a few hole-like defects are present on the surface (Fig. 10b).

4. Conclusion

1. 2-Mercaptobenzothiazole (MBT) has a considerable inhibition effect on the corrosion of steel in 1 M HCl solution. Its inhibition efficiency is proportional to concentration. The high inhibition efficiencies of thiazole derivatives attributed to adherent adsorption of the inhibitor molecules on the metal surface.

2. The potentiodynamic polarization curves indicate that MBT inhibits both cathodic hydrogen evolution reactions and anodic metal dissolution. So it behaves as a mixed type corrosion inhibitor.

3. Langmuir adsorption isotherm best fits with experimental data. The value of $\Delta G^{\circ}_{\mathrm{ads}}$ close to $-40\,\mathrm{kJ\,mol^{-1}}$ is an evidence that the adsorption of inhibitor occurs through charge sharing or transfer from the inhibitor molecules to the metal surface to form a coordinate covalent bond (chemisorption).

4. Gibbs free energy, entropy and enthalpy of adsorption indicate that the adsorption process is spontaneous, increases disorders, endothermic and the molecules are adsorbed on the metal surface by the process of chemisorption.

5. Surface studies show that the surface of sample in solution with inhibitor molecules looks more flat and more uniform with lower roughness than that in the uninhibited solution.

References

[1] Kozuh, S., Gojic, M., Vrasalovic, L., Ivkovic, B.: Kovove Mater., *51*, 2013, p. 53. doi: 10.4149/km_2013_1_53
[2] El-Sayed, A. R., Mohran, H. S., Abd El-Lateef, H. M.: Corros. Sci., *52*, 2010, p. 1976. doi:10.1016/j.corsci.2010.02.029
[3] Gojic, M., Kosec, L.: Kovove Mater., *40*, 2002, p. 222.
[4] Danaee, I., Ghasemi, O., Rashed, G. R., Rashvand Avei, M., Maddahy, M. H.: J. Mol. Struct., *1035*, 2013, p. 247. doi:10.1016/j.molstruc.2012.11.013
[5] Ebenso, E. E., Alemu, H., Umoren, S. A., Obot, I. B.: Int. J. Electrochem. Sci., *3*, 2008, p. 1325.
[6] Ghasemi, O., Danaee, I., Rashed, G. R., Rashvand Avei, M., Maddahy, M. H.: J. Mater. Eng. Perform., *22*, 2013, p. 1054. doi:10.1007/s11665-012-0348-3
[7] Negm, N. A., Ghuiba, F. M., Tawfik, S. M.: Corros. Sci., *53*, 2011, p. 3566. doi:10.1016/j.corsci.2011.06.029
[8] Naqvi, I., Saleemi, A. R., Naveed, S.: Int. J. Electrochem. Sci., *6*, 2011, p. 146.

[9] Danaee, I., Niknejad Khomami, M.: Material Wiss. Werkst., *43*, 2012, p. 942. doi:10.1002/mawe.201200020
[10] Al-Sarawy, A. A., Fouda, A. S., Shehab El-Dein, W. A.: Desalination, *229*, 2008, p. 279. doi:10.1016/j.desal.2007.09.013
[11] Shanbhag, A. V., Venkatesha, T. V., Prabhu, R. A., Praveen, B. M.: Bull. Mater. Sci., *34*, 2011, p. 571. doi:10.1007/s12034-011-0057-9
[12] Danaee, I., Noori, S.: Int. J. Hydrogen Energy, *36*, 2011, p. 12102. doi:10.1016/j.ijhydene.2011.06.106
[13] Macdonald, J. R.: Solid State Ion., *13*, 1984, p. 147. doi:10.1016/0167-2738(84)90049-3
[14] Behpour, M., Ghoreishi, S. M., Soltani, N., Salavati-Niasari, M.: Corros. Sci., *51*, 2009, p. 1073. doi:10.1016/j.corsci.2009.02.011
[15] Musa, A. Y., Kadhum, A. A. H., Mohamad, A. B., Takriff, M. S.: Corros. Sci., *52*, 2010, p. 3331. doi:10.1016/j.corsci.2010.06.002
[16] Döner, A., Solmaz, R., Özcan, M., Kardas, G.: Corros. Sci., *53*, 2011, p. 2902. doi:10.1016/j.corsci.2011.05.027
[17] Danaee, I., Niknejad Khomami, M., Attar, A. A.: J. Mater. Sci. Technol., *29*, 2013. p. 89. doi:10.1016/j.jmst.2012.11.013
[18] Ghasemi, O., Danaee, I., Rashed, G. R., Rashvand Avei, M., Maddahy, M. H.: J. Cent. South Univ., *20*, 2013, p. 301. doi:10.1007/s11771-013-1488-9
[19] Migahed, M. A., Nassar, I. F.: Electrochim. Acta, *53*, 2008, p. 2877. doi:10.1016/j.electacta.2007.10.070
[20] Amin, M. A., Abd El-Rehim, S. S., El-Sherbini, E. E. F., Bayyomi, R. S.: Electrochim. Acta, *52*, 2007, p. 3588. doi:10.1016/j.electacta.2006.10.019
[21] Labjar, N., Lebrini, M., Bentiss, F., Chihib, N. E., El Hajjaji, S., Jama, C.: Mater. Chem. Phys., *119*, 2010, p. 330. doi:10.1016/j.matchemphys.2009.09.006
[22] Veloz, M. A., González, I.: Electrochim. Acta, *48*, 2002, p. 135. doi:10.1016/S0013-4686(02)00549-2
[23] Sherif, E. M., Park, S. M.: Electrochim. Acta, *51*, 2006, p. 1313. doi:10.1016/j.electacta.2005.06.018
[24] Danaee, I., Niknejad Khomami, M., Atar, A. A.: Mater. Chem. Phys., *135*, 2010, p. 658. doi:10.1016/j.matchemphys.2012.05.041
[25] Danaee, I.: Electroanal. Chem., *662*, 2011, p. 415. doi:10.1016/j.jelechem.2011.09.012
[26] Lebrini, M., Lagrenée, M., Vezin, H., Traisnel, M., Bentiss, F.: Corros. Sci., *49*, 2007, p. 2254. doi:10.1016/j.corsci.2006.10.029
[27] Hsu, C. H., Mansfeld, F.: Corrosion, *57*, 2001, p. 747. doi:10.5006/1.3280607
[28] Tamil Sevil, S., Raman, V., Rajendran, N.: Appl. Electrochem., *33*, 2003, p. 1175. doi:10.1023/B:JACH.0000003852.38068.3f
[29] Outirite, M., Lagrenee, M., Lebrini, M., Traisnel, M., Jama, C., Vezin, H., Bentiss, F.: Electrochim. Acta, *55*, 2010, p. 1670. doi:10.1016/j.electacta.2009.10.048
[30] Negm, N. A., El Sabagh, A. M., Migahed, M. A., Abdel Bary, H. M., El Din, H. M.: Corros. Sci., *52*, 2010, p. 2122. doi:10.1016/j.corsci.2010.02.044
[31] Betiss, F., Lebrini, M., Lagrenee, M.: Corros. Sci., *47*, 2005, p. 2915. doi:10.1016/j.corsci.2005.05.034
[32] Ghanbari, A., Attar, M. M., Mahdavian, M.: Mater. Chem. Phys., *124*, 2010, p. 1205. doi:10.1016/j.matchemphys.2010.08.058
[33] Aljourani, J., Raeissi, K., Golozar, M. A.: Corros. Sci., *51*, 2009, p. 1836. doi:10.1016/j.corsci.2009.05.011
[34] Cardoso, S. P., Reis, F. A., Massapust, F. C., Costa, J. F., Tebaldi, L. S., Araújo, L. F. L., Silva, M. V. A., Oliveira, T. S., Gomes, J. A. C. P., Hollauer, E.: Quim. Nova, *28*, 2005, p. 756. doi:10.1590/S0100-40422005000500004
[35] Solmaz, R., Kardas, G., Çulha, M., Yazici, B., Erbil, M.: Electrochim. Acta, *53*, 2008, p. 5941. doi:10.1016/j.electacta.2008.03.055
[36] Avci, G.: Colloids and Surfaces A: Physicochemical and Engineering Aspect, *317*, 2008, p. 730. doi:10.1016/j.colsurfa.2007.12.009
[37] Niknejad Khomami, M., Danaee, I., Attar, A. A., Peykari, M.: Trans. Indian Inst. Met., *65*, 2012, p. 303. doi:10.1007/s12666-012-0134-9
[38] Radovici, O.: In: Proceedings of the 2nd European Symposium on Corrosion inhibitors. Ferrara, Italy, 1965, p. 178.
[39] Begum, A. S., Mallika, J., Gayathri, P.: E-Journal of Chemistry, *7*, 2010, p. 185. doi:10.1155/2010/623298
[40] Szauer, T., Brand, A.: Electrochim. Acta, *26*, 1981, p. 1219. doi:10.1016/0013-4686(81)85102-X
[41] Martinez, S., Stern, I.: Appl. Surf. Sci., *199*, 2002, p. 83. doi:10.1016/S0169-4332(02)00546-9
[42] Ebenso, E. E., Obot, I. B.: Int. J. Electrochem. Sci., *5*, 2010, p. 2012.
[43] Noor, E. A.: Int. J. Electrochem. Sci., *2*, 2007, p. 996.
[44] Shukla, S. K., Ebenso, E. E.: Electrochem. Sci., *6*, 2011, p. 3277.
[45] Bentiss, F., Lebrini, M., Lagrenée, M.: Corros. Sci., *47*, 2005, p. 2915. doi:10.1016/j.corsci.2005.05.034
[46] Noor, E. A., Al-Moubaraki, A. H.: Mater. Chem. Phys., *110*, 2008, p. 145. doi:10.1016/j.matchemphys.2008.01.028